

## **Thermophysical Properties of Quinoline as a Function of Temperature (303–503 K) and Pressure (0.1–400 MPa)**

**S. L. Randzio,<sup>1</sup> D. J. Eatough,<sup>2</sup> E. A. Lewis,<sup>2</sup> and L. D. Hansen<sup>2, 3</sup>**

*Received May 15, 1995*

---

Measured and derived thermophysical properties of quinoline are reported for pressures up to 400 MPa at temperatures from 303 to 503 K. The specific volume at 353 K was determined from the specific volume at atmospheric pressure measured by pycnometry and from isothermal compressibilities measured as a function of pressure up to 400 MPa. Specific volumes, isothermal compressibilities, thermal coefficients of pressure, and isobaric and isochoric heat capacities at pressures up to 400 MPa are derived at several temperatures. The effects of pressure on the isobaric heat capacity of quinoline, a weakly self-associated liquid, are discussed and compared with the pressure effects on heat capacities of *n*-hexane and *m*-cresol.

---

**KEY WORDS:** heat capacity; isobaric thermal expansivity; isothermal compressibility; pressure-scanning calorimetry; quinoline; specific volume; thermal coefficient of pressure.

### **1. INTRODUCTION**

As part of an effort to establish sets of reliable thermophysical data for various liquids over large ranges of temperature and pressure, the present paper reports data for liquid quinoline. Previous papers presented data for *n*-hexane [1], an example of a liquid without strong specific intermolecular interactions, and for *m*-cresol [2], a self-associated liquid. Quinoline is only weakly self-associated, but forms strong complexes with acids such as *m*-cresol [3, and references therein]. Quinoline is an important component

---

<sup>1</sup> Institute of Physical Chemistry, Polish Academy of Sciences, ul. Kasprzaka 44/52, 01-224 Warsaw, Poland.

<sup>2</sup> Department of Chemistry, Brigham Young University, Provo, Utah 84602, U.S.A.

<sup>3</sup> To whom correspondence should be addressed.

of the basic fraction of coal liquids and a key nitrogen-containing compound in heavy petroleum, shale oil and tar sands. One of the problems in upgrading these alternate fuels is removal of organic nitrogen [4, and references therein]. The nitrogen-containing compounds are a potential source of useful materials if they could be readily separated. Accurate data on the thermophysical properties of quinoline may be useful in developing cost-effective methods for such processes. Recent efforts to collect thermodynamic data on quinoline have mostly been studies of thermodynamic properties as a function of temperature under saturation conditions or under only slightly elevated pressures. The saturated vapor pressures [4–10], densities under normal or saturated vapor pressures [4, 11–13], heat of combustion [4, 14], isobaric heat capacities, enthalpies, and derived thermodynamic functions for the solid and liquid phases of quinoline have been reported [4, 15, 16]. Ideal-gas thermodynamic properties have also been reported for quinoline [4].

This study presents results of measurements of isobaric thermal expansivities of quinoline measured from 303.15 to 503.15 K under pressures up to 400 MPa and of specific volumes measured as a function of pressure up to 400 MPa at 353.15 K. Specific volumes, isothermal compressibilities, temperature coefficients of pressure, and isobaric and isochoric heat capacities for the pressure range up to 400 MPa are derived from these data and from literature data on the isobaric heat capacity at atmospheric or saturation vapor pressure. The pressure effects on the heat capacity of quinoline are emphasized in the present study and compared with pressure effects on the heat capacity of *n*-hexane and *m*-cresol.

## 2. EXPERIMENTS

Measurements of thermal expansivities were made by stepwise pressure-scanning with an instrument previously described [17]. Calorimetric determination of thermal expansivities is based on the relation

$$\alpha - \alpha_{p,ss} = -kI/(T \Delta p) \quad (1)$$

where  $k(\text{MPa} \cdot \text{V}^{-1} \cdot \text{s}^{-1})$  is a temperature-dependent calibration constant as given in a previous paper [17],  $I(\text{V} \cdot \text{s})$  is the time integral of the calorimetric signal (heat rate) resulting from the calorimeter response to the pressure step  $\Delta p(\text{MPa})$  performed under quasi-isothermal conditions,  $\alpha_{p,ss}(5.1 \times 10^{-5} \text{K}^{-1})$  is the thermal expansivity of the stainless steel of the calorimeter vessel, and  $T(\text{K})$  is the absolute temperature.

To prevent sorption of moisture, the quinoline was kept under argon, transferred with a syringe, and immediately injected into the calorimetric

vessel, which was rapidly closed with a cone and cone-retaining gland in such a way that no vapor space was present. After pressurizing to the highest pressure, the system was allowed to equilibrate thermally and mechanically for a few hours before measurements began. Measurements were made with decreasing pressure.

Measurements of the specific volume of quinoline as a function of pressure were done with the calorimeter pressure generator as previously described [17]. The measurements reported in this study were made with an instrument built in Warsaw [18]. The pressure generator in this instrument is driven with a stepping motor and automatically records pressure and the number of motor steps. The rate of volume change was kept small ( $\approx 1 \times 10^{-4} \text{cm}^3 \cdot \text{s}^{-1}$ ) to make the effect of the heat of compression on the pressure readings negligible. Occasionally the program was stopped to verify that the measuring system was at thermal and mechanical equilibrium. Calibration of the pressure generating system for the volume measurements was done with *n*-hexane for which the volume at these pressure and temperature conditions is believed to be accurate to better than  $\pm 0.2\%$  [1]. The static calibration found was  $(5.838 \pm 0.014) \times 10^{-6} \text{cm}^3$  per motor sep. The full-scale resolution in the measurements of compressibilities by counting the number of motor steps was  $\pm 2$  ppm [16].

The specific volume of quinoline at 353.15 K under atmospheric pressure was measured with a pycnometer calibrated with water. The precision of the volume measurements under atmospheric pressure was  $\pm 0.2\%$ .

The quinoline used in this study was obtained from Aldrich, #25,401.0,99 + %, used without further purification.

### 3. RESULTS

#### 3.1. Isobaric Coefficient of Thermal Expansion, $\alpha_p$

Isobaric thermal expansivities measured at 303.15, 353.15, 403.15, 453.15, and 503.15 K are given in Table I. Pressure values given in Table I are the mean pressures at the beginning and end of a pressure step. The end values were measured at the end of the thermogram, after thermal and mechanical equilibrium was reestablished. Each ending pressure became the beginning pressure for the next step. The isothermal solid-liquid transition was observed at 303.15 K as large changes in  $\alpha_p$  values, above about 160 MPa. Values obtained with both phases present are equal to a weighted sum of the thermal expansivities of solid and liquid quinoline plus the entropy change of the phase transition. The entropy change of the phase transition is the largest term in the sum.

**Table I.** Results of Pressure-Scanning Calorimetric Measurements of Isobaric Thermal Expansivity of Quinoline

$p$ (MPa)	$\Delta p^a$ (MPa)	$\alpha_p$ ( $10^{-4} \text{ K}^{-1}$ )	$p$ (MPa)	$\Delta p$ (MPa)	$\alpha_p$ ( $10^{-4} \text{ K}^{-1}$ )
$T = 303.15 \text{ K}$					
342.9	18.06	$4.91 \pm 0.18$	223.6	7.86	$12.73 \pm 0.51$
324.5	18.75	$5.58 \pm 0.20$	206.0	27.47	$10.54 \pm 0.30$
301.2	27.92	$8.09 \pm 0.25$	178.3	27.92	$5.37 \pm 0.18$
277.4	19.72	$13.90 \pm 0.41$	127.1	27.99	$5.46 \pm 0.18$
257.7	19.72	$27.63 \pm 0.77$	76.72	22.48	$6.09 \pm 0.20$
243.3	9.10	$61.33 \pm 2.16$	51.5	27.99	$6.46 \pm 0.21$
232.6	10.20	$61.23 \pm 2.05$	28.4	18.13	$6.64 \pm 0.23$
$T = 353.15 \text{ K}$					
236.7	25.79	$4.74 \pm 0.10$	86.1	19.58	$6.06 \pm 0.13$
210.4	26.89	$4.95 \pm 0.11$	65.8	20.82	$6.45 \pm 0.13$
181.6	30.61	$5.17 \pm 0.11$	45.6	19.58	$6.92 \pm 0.14$
153.8	24.96	$5.49 \pm 0.11$	27.2	17.24	$7.23 \pm 0.15$
129.7	23.30	$5.54 \pm 0.12$	10.2	16.89	$7.64 \pm 0.16$
106.7	21.72	$5.73 \pm 0.12$			
$T = 403.15 \text{ K}$					
315.4	23.51	$4.18 \pm 0.10$	120.0	25.03	$5.58 \pm 0.11$
262.1	29.92	$4.39 \pm 0.10$	96.1	22.68	$5.83 \pm 0.12$
233.0	28.27	$4.50 \pm 0.10$	74.6	20.83	$6.10 \pm 0.13$
198.7	27.44	$4.89 \pm 0.10$	53.2	22.48	$6.79 \pm 0.13$
172.3	25.30	$5.08 \pm 0.11$	31.3	21.30	$7.03 \pm 0.14$
146.1	27.17	$5.26 \pm 0.11$	10.8	19.86	$7.58 \pm 0.15$
$T = 453.15 \text{ K}$					
319.5	19.93	$4.01 \pm 0.13$	181.9	25.92	$4.74 \pm 0.13$
296.8	25.51	$4.00 \pm 0.12$	153.4	31.03	$5.04 \pm 0.13$
272.4	26.06	$4.15 \pm 0.12$	123.5	28.82	$5.31 \pm 0.14$
259.4	27.72	$4.19 \pm 0.12$	94.8	28.61	$5.82 \pm 0.15$
245.5	27.72	$4.25 \pm 0.12$	67.8	25.30	$6.38 \pm 0.16$
234.8	25.92	$4.20 \pm 0.12$	42.4	25.58	$6.97 \pm 0.17$
208.5	26.82	$4.46 \pm 0.13$	19.2	20.20	$7.87 \pm 0.20$
$T = 503.15 \text{ K}$					
323.6	21.72	$3.63 \pm 0.14$	126.5	24.82	$5.14 \pm 0.17$
300.7	24.20	$3.73 \pm 0.14$	102.2	23.10	$5.68 \pm 0.18$
251.6	24.82	$3.84 \pm 0.14$	79.9	21.30	$6.19 \pm 0.20$
225.6	27.16	$4.06 \pm 0.14$	58.3	22.06	$6.77 \pm 0.21$
200.4	23.17	$4.37 \pm 0.15$	31.3	21.44	$7.70 \pm 0.23$
176.9	23.86	$4.51 \pm 0.16$	13.4	14.41	$8.24 \pm 0.27$
152.0	26.06	$4.72 \pm 0.16$			

<sup>a</sup> See Eq. (1).

The accuracy limits given in Table I are the estimated maximal errors determined from uncertainties in the measured pressures ( $\pm 0.14$  MPa), integrals (I in Eq. (1),  $\pm 0.2\%$ ), temperature ( $\pm 0.1$  K),  $\alpha_{p,ss}$  ( $\pm 10\%$ ), and calibration constant ( $k$  in Eq. (1), from  $\pm 0.4$  to  $1.7\%$  depending on temperature [17]).

The results on the liquid phase were fitted by least squares to Eqs. (2)–(4)

$$\alpha_p(p, T) = [a(T)][b(T) + p]^{-0.5} \tag{2}$$

where

$$a(T) = a_0 + a_1 T + a_2 T^2 \tag{3}$$

and

$$b(T) = a_0 + a_1 T + a_2 T^2 \tag{4}$$

with the resulting coefficients given in Table II with pressure expressed in MPa and temperature in kelvins. The standard deviation of the difference between the experimental data points and the values calculated from Eqs. (2)–(4) is  $\pm 1.9\%$  and the errors are randomly distributed. Calculated  $\alpha_p$  values at 353.15, 403.15, 453.15, and 503.15 K as well as part of the experimental data at 303.15 K are presented in Fig. 1. The estimated uncer-

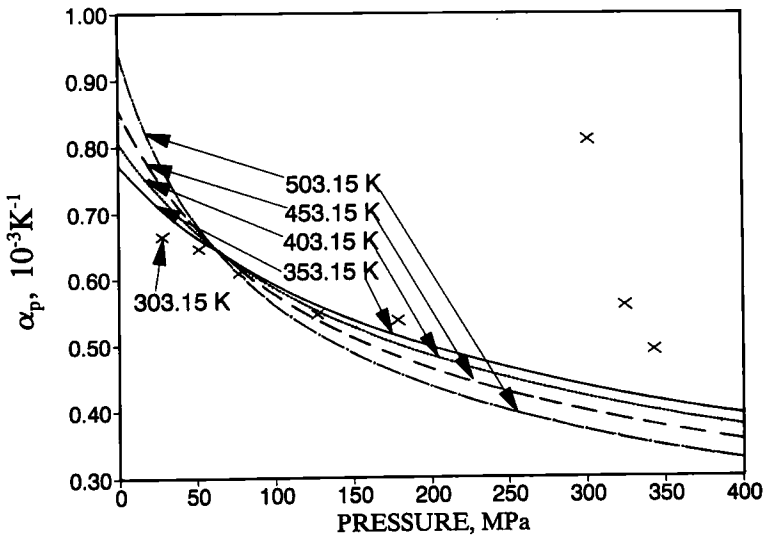


Fig. 1. Isobaric thermal expansivity ( $\alpha_p$ ) of quinoline calculated with Eqs. (2)–(4) at 353.15 to 503.15 K and with Eq. (1) at 303.15 K.

Table II. Values of Coefficients in Eqs. (3), (4), (7), and (12) for Liquid Quinoline

Eq.	$a_0$	$a_1$	$a_2$	$a_3$
3	$1.112 \times 10^{-2} \text{ MPa}^{-1/2} \cdot \text{K}^{-1}$	$7.887186 \times 10^{-7} \text{ MPa}^{-1/2} \cdot \text{K}^{-2}$	$-1.802655 \times 10^{-8} \text{ MPa}^{-1/2} \cdot \text{K}^{-3}$	—
4	361.5 MPa	$-0.662977 \text{ MPa} \cdot \text{K}^{-1}$	$1.027818 \times 10^{-4} \text{ MPa} \cdot \text{K}^{-2}$	—
7	21.4398	-8288.64 K	$-0.01981 \text{ K}^{-1}$	$1.0086 \times 10^{-5} \text{ K}^{-2}$
12	$0.8971075 \text{ kJ} \cdot \text{K}^{-1} \cdot \text{kg}^{-1}$	$0.087799227 \text{ kJ} \cdot \text{K}^{-1} \cdot \text{kg}^{-1} \cdot \text{cK}^{-1}$	$0.053791127 \text{ kJ} \cdot \text{K}^{-1} \cdot \text{kg}^{-1} \cdot \text{cK}^{-2}$	$-4.7879579 \times 10^{-3} \text{ kJ} \cdot \text{K}^{-1} \cdot \text{kg}^{-1} \cdot \text{cK}^{-3}$

tainty in the calculated  $\alpha_p$  values is  $\pm 0.7\%$ . The unique crossing point of the isotherms of the isobaric thermal expansivity of quinoline at  $60 \pm 0.4$  MPa demonstrates a behaviour closer to that of *n*-hexane [1] than of *m*-cresol [2]. However, the temperature dependence of the thermal expansivity of quinoline at high pressures is larger than that for *n*-hexane at the same temperatures.

### 3.2. Specific Volume, $v(p, T)$

The specific volumes of liquid quinoline measured at 353.15 K and at various pressures are given in Table III, column 2. The data in column 2 are derived from pycnometric measurements at atmospheric pressure and compressibility measurements as a function of pressure. Note that experimental measurements of compressibility were made only at 353.15 K. Equation (5) was fitted to the specific volume data at 353.15 K by the least-squares method,

$$v(T_R, p) = v_0 \{1 - C \ln[(B + p)/(B + 0.1013)]\} \quad (5)$$

with  $p$  expressed in MPa,  $v_0 = 0.9541 \text{ cm}^3 \cdot \text{g}^{-1}$ ,  $B = 126.649$ , and  $C = 0.086219$ . The standard deviation of the differences between the experimental data points and values calculated from Eq. (5) is 0.003%, with the deviations being randomly distributed.  $T_R = 353.15$  K was taken as the reference temperature and  $v(T_R, p)$  as the reference volume isotherm for derivation of further thermodynamic quantities for the liquid phase of quinoline.

The specific volumes of liquid quinoline from standard atmospheric pressure (0.1013 MPa) up to 400 MPa and from 353.15 to 503.15 K were obtained from Eq. (6) with thermal expansivities from Eqs. (2)–(4) and the specific volume isotherm at 353.15 K from Eq. (5),

$$v(T, p) = v(T_R, p) \exp \left[ \int_{T_R}^T \alpha_p dT \right] \quad (6)$$

The saturation vapor pressure ( $p_s$ ) from 353.15 to 503.15 K was obtained by least-squares fit of Eq. (7) to vapor pressure data in Refs. 4, 6–8,

$$p_s = \exp(a_0 + a_1 T^{-1} + a_2 T + a_3 T^2) \quad (7)$$

The values of the coefficients giving  $p_s$  in MPa are given in Table II. The standard deviation of the differences between the experimental data points and the values calculated from Eq. (7) is  $\pm 0.4\%$ , with the deviations being randomly distributed. Specific volumes calculated at three temperatures are given in Table III, columns 3–5.

Table III. Specific Volume ( $1000 \text{ m}^3 \cdot \text{kg}^{-1}$ ) of Liquid Quinoline

$p$ (MPa)	$T$ (K)			
	353.15	403.15	453.15	503.15
$p_s$	0.9541	0.9925	1.0346	1.0820
10	0.9479	0.9846	1.0243	1.0681
20	0.9421	0.9773	1.0149	1.0556
30	0.9367	0.9705	1.0063	1.0445
40	0.9316	0.9641	0.9984	1.0344
50	0.9268	0.9582	0.9910	1.0253
60	0.9223	0.9527	0.9842	1.0168
70	0.9180	0.9474	0.9778	1.0090
80	0.9139	0.9425	0.9718	1.0017
90	0.9100	0.9378	0.9662	0.9949
100	0.9063	0.9333	0.9609	0.9886
110	0.9027	0.9291	0.9558	0.9826
120	0.8993	0.9250	0.9510	0.9769
130	0.8961	0.9212	0.9464	0.9716
140	0.8929	0.9175	0.9421	0.9665
150	0.8899	0.9139	0.9379	0.9616
160	0.8870	0.9105	0.9339	0.9570
170	0.8841	0.9072	0.9301	0.9526
180	0.8814	0.9040	0.9264	0.9483
190	0.8788	0.9009	0.9228	0.9443
200	0.8762	0.8979	0.9194	0.9404
210	0.8737	0.8951	0.9161	0.9366
220	0.8713	0.8923	0.9130	0.9330
230	0.8690	0.8896	0.9099	0.9295
240	0.8667	0.8870	0.9069	0.9261
250	0.8645	0.8844	0.9040	0.9229
260	0.8624	0.8820	0.9012	0.9197
270	0.8603	0.8796	0.8985	0.9167
280	0.8582	0.8772	0.8958	0.9137
290	0.8562	0.8750	0.8933	0.9108
300	0.8543	0.8727	0.8908	0.9081
310	0.8524	0.8706	0.8884	0.9053
320	0.8505	0.8685	0.8860	0.9027
330	0.8487	0.8664	0.8837	0.9001
340	0.8469	0.8644	0.8814	0.8976
350	0.8451	0.8624	0.8792	0.8952
360	0.8434	0.8605	0.8771	0.8928
370	0.8418	0.8586	0.8750	0.8905
380	0.8401	0.8568	0.8729	0.8883
390	0.8385	0.8550	0.8709	0.8561
400	0.8369	0.8532	0.8690	0.8839



Table IV. Coefficients  $B$  and  $C$  of the Tait Eq. (8) for Quinoline

$T$ (K)	$B$ (MPa)	$C$	SD (%)	Average deviation (%)
353.15	126.649	0.086219	0.00	0.000
403.15	106.135	0.089959	0.01	0.001
453.15	86.021	0.092632	0.01	0.002
503.15	66.242	0.094064	0.02	0.002

### 3.3. Coefficient of Isothermal Compressibility, $\kappa_T$

Isothermal compressibilities were calculated with a form of the Tait equation, Eq. (8), at selected temperatures from 353.15 to 503.15 K at pressures from the saturated vapor pressure up to 400 MPa.

$$\kappa_T = C / \{ (B + p) \{ 1 - C \ln[(B + p)/(B + p_s)] \} \} \quad (8)$$

Table IV gives the values of the coefficients  $B$  and  $C$  obtained by fitting the specific volume data in Table III. Table IV also gives standard and average deviations of the differences between the specific volumes derived with Eqs. (5) and (6) and the volumes obtained with the Tait equation at each tem-

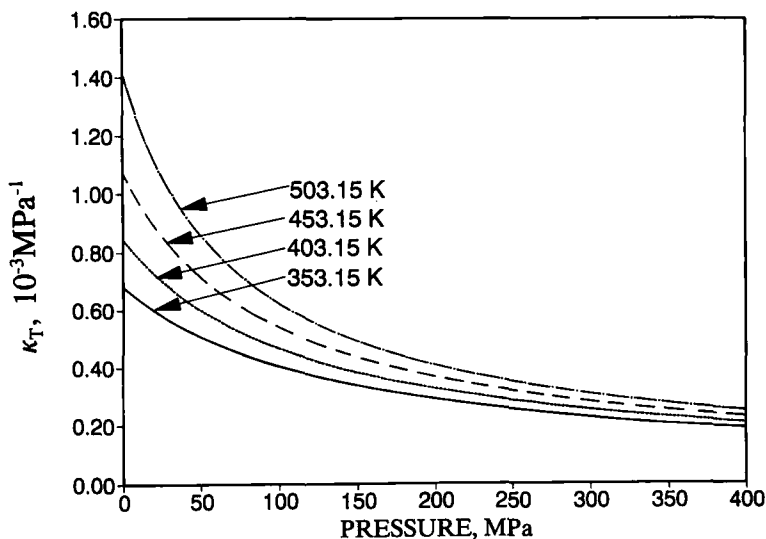


Fig. 2. Isothermal compressibility ( $\kappa_T$ ) of liquid quinoline calculated with Eq. (8).

perature. A graphic presentation of isothermal compressibilities at selected temperatures is given in Fig. 2.

### 3.4. Thermal Coefficient of Pressure, $(\partial p/\partial T)_v$

The thermal coefficient of pressure of liquid quinoline at selected temperatures from 353.15 to 503.15 K at pressures from the saturated vapor pressure up to 400 MPa was calculated with Eq. (9),

$$(\partial p/\partial T)_v = \alpha_p/\kappa_T \quad (9)$$

A graphic presentation of selected isotherms is given in Fig. 3. Numerical values for  $(\partial p/\partial T)_v$  can be obtained from values for  $\alpha_p$  from Eqs. (2)–(4) and values for  $\kappa_T$  from Eq. (8).

### 3.5. Specific Isobaric Heat Capacity

The effects of pressure on the specific isobaric heat capacity of liquid quinoline at selected temperatures were calculated with Eq. (10),

$$\Delta_{p_0}^p C_{p,T}^1(p) = -T \int_{p_0}^p v(p, T) [\alpha_p^2 + (\partial \alpha_p/\partial T)_p] dp \quad (10)$$

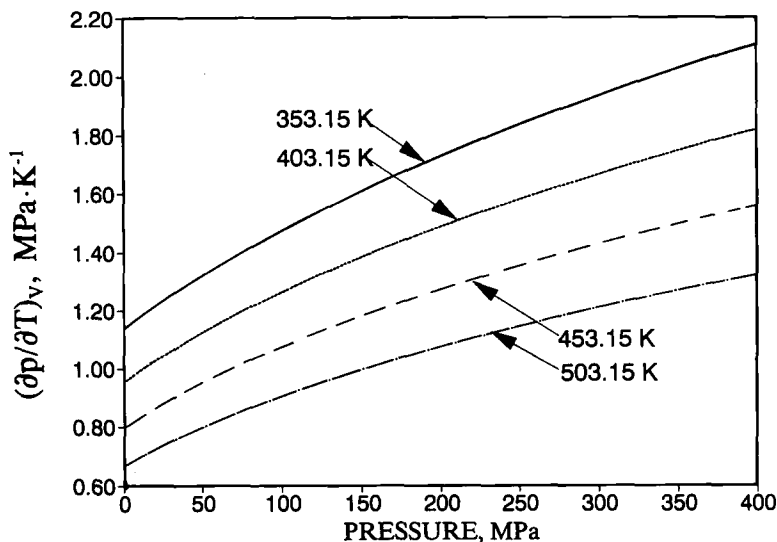


Fig. 3. Thermal coefficient of pressure  $(\partial p/\partial T)_v$  of liquid quinoline calculated with Eq. (9).

Table V. Pressure Effects on Isobaric Specific Heat Capacity of Liquid Quinoline,  $\Delta_{p_0}^p C_{p,T}^l(p)$ , in  $\text{kJ} \cdot \text{K}^{-1} \cdot \text{kg}^{-1}$

$p$ (MPa)	$T$ (K)			
	353.15	403.15	453.15	503.15
10	-0.004	-0.005	-0.008	-0.015
20	-0.007	-0.010	-0.014	-0.026
30	-0.010	-0.013	-0.019	-0.034
40	-0.012	-0.016	-0.023	-0.039
50	-0.014	-0.019	-0.026	-0.043
60	-0.016	-0.021	-0.028	-0.045
70	-0.018	-0.022	-0.030	-0.047
80	-0.019	-0.024	-0.031	-0.048
90	-0.020	-0.025	-0.032	-0.048
100	-0.022	-0.026	-0.032	-0.048
110	-0.022	-0.026	-0.032	-0.048
120	-0.023	-0.027	-0.032	-0.047
130	-0.024	-0.027	-0.032	-0.046
140	-0.024	-0.027	-0.032	-0.045
150	-0.025	-0.027	-0.031	-0.043
160	-0.025	-0.027	-0.031	-0.042
170	-0.026	-0.027	-0.030	-0.040
180	-0.026	-0.027	-0.029	-0.038
190	-0.026	-0.027	-0.028	-0.036
200	-0.026	-0.026	-0.027	-0.034
210	-0.026	-0.026	-0.026	-0.032
220	-0.026	-0.026	-0.025	-0.030
230	-0.026	-0.025	-0.024	-0.028
240	-0.026	-0.025	-0.023	-0.026
250	-0.026	-0.024	-0.022	-0.024
260	-0.026	-0.024	-0.020	-0.022
270	-0.026	-0.023	-0.019	-0.019
280	-0.025	-0.022	-0.018	-0.017
290	-0.025	-0.022	-0.016	-0.015
300	-0.025	-0.021	-0.015	-0.013
310	-0.025	-0.020	-0.014	-0.010
320	-0.024	-0.019	-0.012	-0.008
330	-0.024	-0.019	-0.011	-0.006
340	-0.024	-0.018	-0.009	-0.004
350	-0.023	-0.017	-0.008	-0.001
360	-0.023	-0.016	-0.006	0.001
370	-0.023	-0.015	-0.005	0.003
380	-0.022	-0.014	-0.004	0.005
390	-0.022	-0.014	-0.002	0.008
400	-0.021	-0.013	-0.001	0.010

Standard atmospheric pressure,  $p_0 = 0.1013$  MPa, was taken as the lower limit of integration instead of the saturation pressure  $p_s$ , because the high-temperature limit of the experimental data, 503.15 K, is below the boiling temperature of quinoline, 511.2 K [19]. The correction for this difference is negligible. Values of  $v(p, T)$  were calculated with Eqs. (5) and (6),  $\alpha_p$  values with Eqs. (2)–(4), and  $(\partial\alpha_p/\partial T)_p$  values with the derivative of Eqs. (2)–(4).  $\Delta_{p_0}^p C_{p,T}^1(p)$  values were then obtained by numerical integration. The results of the calculations are given in Table V.

The specific isobaric heat capacity of liquid quinoline as a function of  $p$  and  $T$  can be calculated with the thermodynamic relation in Eq. (11),

$$C_p^1(p, T) = C_{p,p_s}^1 + \Delta_{p_s}^p C_p^1(p, T) \quad (11)$$

where  $C_{p,p_s}^1$  is the specific isobaric heat capacity of liquid quinoline at the pressure of the saturated vapor. Values of  $C_{p,p_s}^1$  were obtained from Steele et al. [4] and fitted by the least-squares method to Eq. (12),

$$C_{p,p_s}^1(T) = a_0 + a_1 g + a_2 g^2 + a_3 g^3 \quad (12)$$

where  $g = T/100$ , and the coefficients obtained are given in Table II. The standard deviation of the differences between the values obtained from Eq. (12) and the literature data is  $\pm 0.06\%$  and the deviations are randomly distributed. The specific isobaric heat capacities derived with Eqs. (11) and

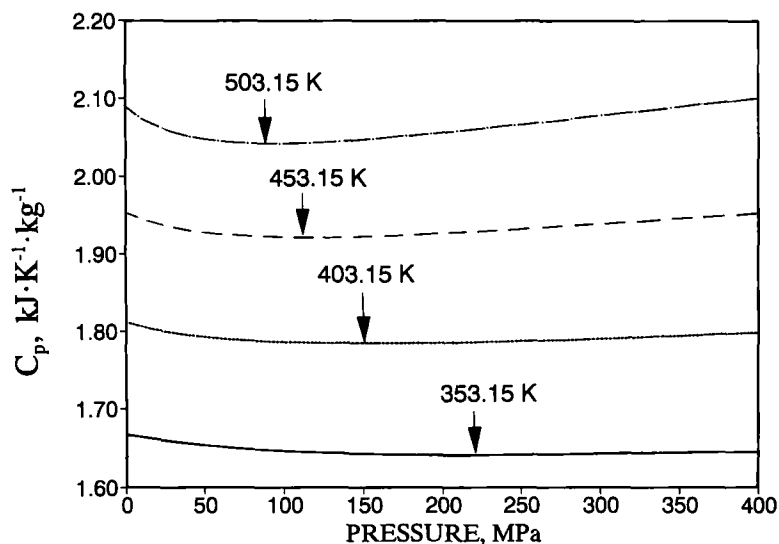


Fig. 4. Isobaric specific heat capacity of liquid quinoline calculated with Eqs. (11) and (12). Vertical arrow points indicate minima.

(12) for pressures up to 400 MPa and at 353.15, 403.15, 453.15, and 503.15 K are given in Fig. 4.

### 3.6. Specific Isochoric Heat Capacity, $C_V^1$

The specific isochoric heat capacity of liquid quinoline at selected temperatures as a function of pressure up to 400 MPa was calculated with Eq. (13),

$$C_V^1 = C_p^1 - Tv\alpha_p^2/\kappa_T \quad (13)$$

Values for  $C_p^1$  were derived from data in Table V and Eqs. (11) and (12); values for  $v$  were from Table III, as calculated with Eqs. (5) and (6); values for  $\alpha_p$  were calculated with Eqs. (2)–(4); and values for  $\kappa_T$  with Eq. (8). The resulting values of  $C_V^1$  are presented in Table VI.

### 3.7. Error Analysis

Estimation of the accuracy of the computed values presented in this paper is made difficult by the necessary sequences of fitting, integrating, and differentiating. Thus, an empirical approach has been taken by determining the effect on the calculated values of shifting the input experimental data by a fixed percentage. The results show that the error in the calculated value is proportional to the error in the input data, i.e., there is no significant error amplification by the calculation procedures used in this study [20]. The estimated uncertainties in the data in Tables III, V, and VI are indicated by the number of significant digits listed.

## 4. DISCUSSION

The present volume data obtained at atmospheric pressure can be compared with the data of Steele et al. [4]. The specific volume of quinoline measured at 353.15 K differs by  $-0.28\%$  from the value derived from Steele's equation at this temperature. A plot of the difference between data under atmospheric pressure calculated from Eqs. (5) and (6) and the data of Steele et al. [4] under saturation pressure (presented only as a fitted equation) from 303 to 423 K is given in Fig. 5. The mean of the volume deviations shown in Fig. 5 is  $-0.27\%$ . The root-mean-square error between the experimental data points and the fitting equation of Steele et al. [4] as reported by the authors is  $\pm 0.27\%$ . There are no literature data for comparison with the high-pressure data for the isobaric thermal expansivities and volumes.

Table VI. Specific Isochoric Heat Capacity of Liquid Quinoline,  $C_V^l$ , in  $\text{kJ} \cdot \text{K}^{-1} \cdot \text{kg}^{-1}$ 

$p$ (MPa)	$T$ (K)			
	353.15	403.15	453.15	503.15
$p_s$	1.667	1.812	1.954	2.091
10	1.663	1.806	1.946	2.075
20	1.660	1.802	1.940	2.065
30	1.657	1.798	1.935	2.057
40	1.655	1.795	1.931	2.052
50	1.653	1.793	1.928	2.048
60	1.651	1.791	1.926	2.045
70	1.649	1.789	1.924	2.044
80	1.648	1.788	1.923	2.043
90	1.647	1.787	1.922	2.042
100	1.646	1.786	1.922	2.043
110	1.645	1.785	1.922	2.043
120	1.644	1.785	1.922	2.044
130	1.643	1.785	1.922	2.045
140	1.643	1.784	1.922	2.046
150	1.642	1.784	1.923	2.048
160	1.642	1.784	1.923	2.049
170	1.642	1.784	1.924	2.051
180	1.641	1.785	1.925	2.053
190	1.641	1.785	1.926	2.055
200	1.641	1.785	1.927	2.057
210	1.641	1.785	1.928	2.059
220	1.641	1.786	1.929	2.061
230	1.641	1.786	1.930	2.063
240	1.641	1.787	1.931	2.065
250	1.641	1.787	1.932	2.067
260	1.641	1.788	1.934	2.069
270	1.642	1.789	1.935	2.071
280	1.642	1.789	1.936	2.074
290	1.642	1.790	1.938	2.076
300	1.642	1.791	1.939	2.078
310	1.642	1.792	1.940	2.080
320	1.643	1.792	1.942	2.083
330	1.643	1.793	1.943	2.085
340	1.643	1.794	1.945	2.087
350	1.644	1.795	1.946	2.089
360	1.644	1.795	1.948	2.092
370	1.644	1.796	1.949	2.094
380	1.645	1.797	1.950	2.096
390	1.645	1.798	1.952	2.098
400	1.646	1.799	1.953	2.101

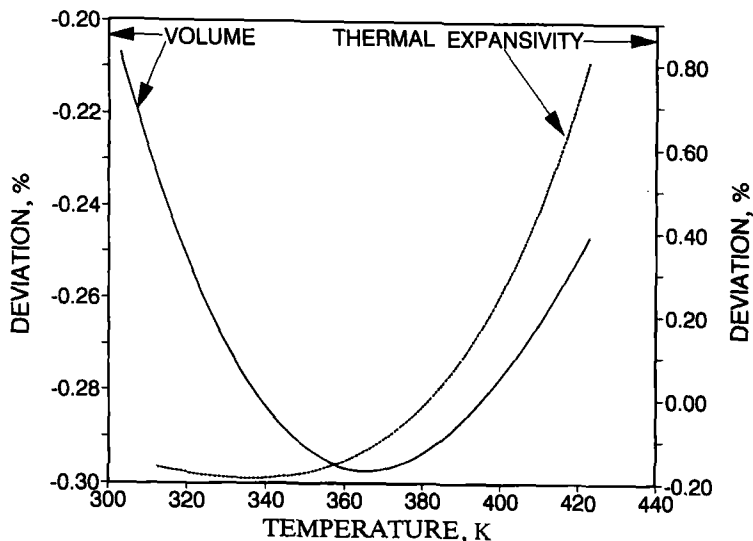


Fig. 5. The difference between our data and data from Steele et al. [4] for specific volumes and isobaric thermal expansivities for liquid quinoline at atmospheric pressure.

A comparison of isobaric thermal expansivities obtained from Eqs. (2)–(4) under atmospheric pressure and thermal expansivities obtained from the equation for liquid densities under saturation pressure from Steele et al. [4] over the temperature interval from 303 to 423 K is given in Fig. 5. The agreement is surprisingly good, better than the claimed precision ( $\pm 2\%$ ) of our experimental method [17].

The behavior of the isobaric thermal expansivity (see Fig. 1) and isobaric heat capacity (see Fig. 4) of liquid quinoline as a function of pressure at various temperatures can be compared with the behavior of *n*-hexane, a model nonassociated liquid [1], and of *m*-cresol, an associated liquid [2]. The thermal expansivity of quinoline behaves more like that of *n*-hexane. Both quinoline and *n*-hexane show a nearly unique crossing point in the isotherms, while *m*-cresol does not. At  $60 \pm 0.4$  MPa for liquid quinoline  $\alpha_p = (6.50 \pm 0.02) \times 10^{-4} \text{K}^{-1}$  over the whole temperature range under study. However, the temperature dependence of  $\alpha_p$  is greater at high pressures and lower at low pressures for quinoline than for *n*-hexane. Also,  $\alpha_p$  for quinoline is significantly smaller than  $\alpha_p$  for *n*-hexane. Thus,  $\partial\alpha_p/\partial T$  is closer to the value of  $\alpha_p$  itself in quinoline than in *n*-hexane and this numerical fact is reflected in differences in the shapes of the isotherms for  $\Delta_{p_s}^p C_{p,T}^1(p)$  [see Eq. (10) and Fig. 6] for quinoline and *n*-hexane. Because

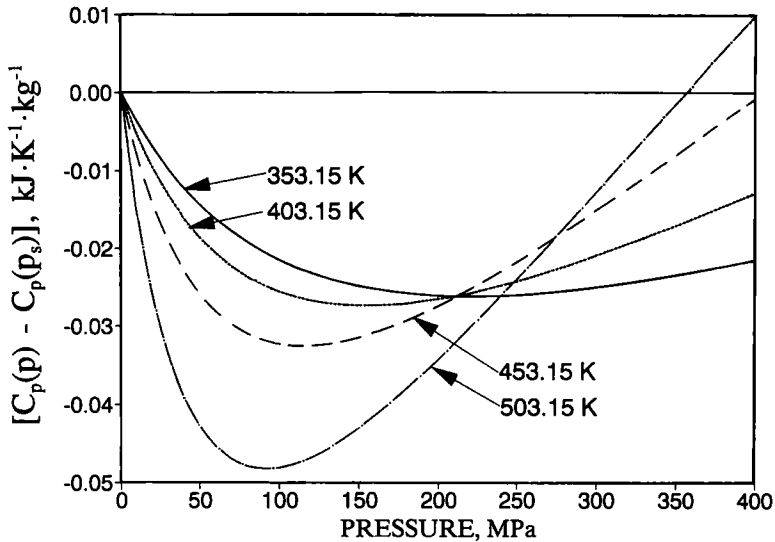


Fig. 6. Isothermal pressure increments of isobaric heat capacity of liquid quinoline calculated with Eq. (10).

$\partial\alpha_p/\partial T$  changes sign at the crossing point,  $\Delta_{p_s}^p C_{p,T}^1(p)$  for quinoline exhibits a minimum which moves to higher pressures as the temperature decreases.

In exhibiting a minimum at all the temperatures covered in this study, the heat capacity of quinoline (see Fig. 4) also behaves more like that for *n*-hexane than like that for *m*-cresol. However, the trend with temperature of the pressure at the minimum in the isotherms of the heat capacity is opposite for quinoline and *n*-hexane. For *n*-hexane the minima appear at higher pressures as the temperature is increased. For quinoline the minimum shifts to lower pressures as the temperature is increased.

Isotherms of the difference between isobaric and isochoric molar heat capacities of liquid quinoline (see Fig. 7) behave more like the isotherms of *n*-hexane than of *m*-cresol, although there is no unique crossing point as was observed for liquid *n*-hexane. The crossing of the isotherms for quinoline moves to higher pressures as the temperature decreases.

The differences between quinoline and *n*-hexane can be explained by assuming that quinoline is weakly associated. The heat capacities are thus the sum of the isobaric heat capacity of unassociated liquid quinoline and a contribution from the enthalpy of association resulting from a shift in the self-association equilibrium. This conclusion is in accord with previous results on the heat of dilution of quinoline in decane at 298.15 K [3] that showed quinoline to be weakly self-associated.



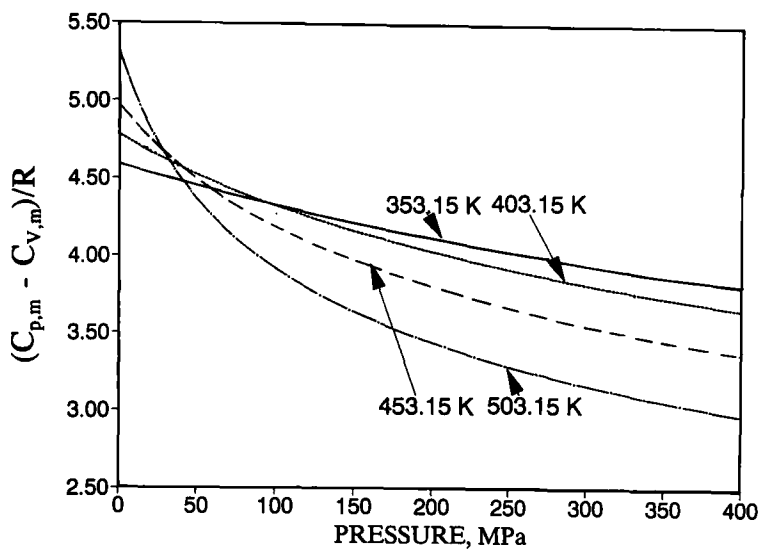


Fig. 7. Isotherms of the difference between isobaric and isochoric molar heat capacities of liquid quinoline.

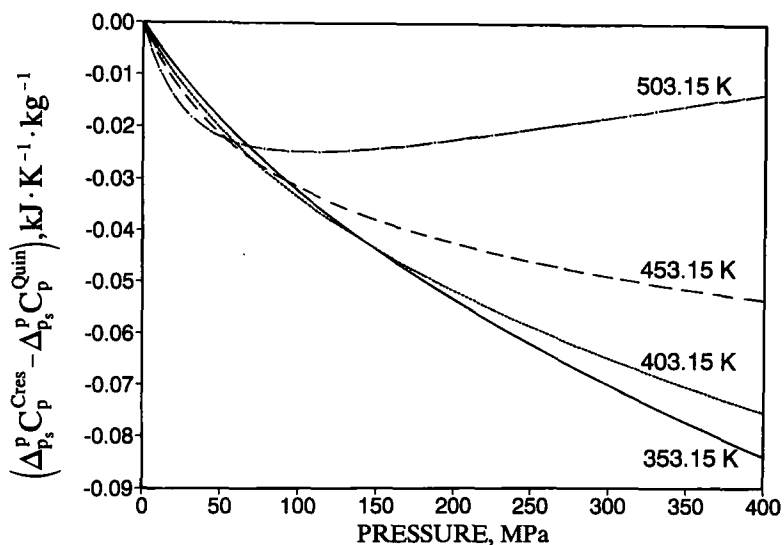


Fig. 8. Isotherms of the difference in the pressure increments of the specific isobaric heat capacity of *m*-cresol vs. quinoline.

Differences in the thermodynamic functions between quinoline and *m*-cresol are a result of the much stronger self-association of *m*-cresol. The difference in the effects of self-association on the specific isobaric heat capacities of *m*-cresol and quinoline is shown in Fig. 8 as an example.

This study provides another set of data that can be used to test predictions of associated liquid models over wide ranges of temperature and pressure.

## ACKNOWLEDGMENT

S.L.R. wishes to express appreciation for the hospitality and financial support received from the Department of Chemistry, Brigham Young University, during his visits there.

## REFERENCES

1. S. L. Randzio, J.-P. E. Grolier, J. R. Quint, D. J. Eatough, E. A. Lewis, and L. D. Hansen, *Int. J. Thermophys.* **15**:415 (1994).
2. S. L. Randzio, E. A. Lewis, D. J. Eatough, and L. D. Hansen, *Int. J. Thermophys.* **16**:883 (1995).
3. D. J. Eatough, S. L. Wolfley, L. J. Dungan, E. A. Lewis, and L. D. Hansen, *J. Energy Fuels* **1**:94 (1987).
4. W. V. Steele, D. G. Archer, R. D. Chirico, W. B. Collier, I. A. Hossenlopp, A. Ngyuen, N. K. Smith, and B. E. Gammon, *J. Chem. Thermodynam.* **20**:1233 (1988).
5. F. Glaser and H. Ruland, *Chem. Ing. Techn.* **29**:722 (1957).
6. S. Malanowski, *Bull. Acad. Pol. Sci. Ser. Sci. Chim.* **9**:71 (1961).
7. C. V. Rostyne and J. M. Prausnitz, *J. Chem. Eng. Data* **25**:1 (1980).
8. G. R. Wilson, R. H. Johnston, S.-C. Hwang, and C. Tsionopulos, *C. Ind. Eng. Chem. Process Des. Dev.* **20**:94 (1981).
9. D. H. Krevor, F. W. Lam, and J. M. Prausnitz, *J. Chem. Eng. Data* **31**:353 (1986).
10. V. G. Niesen and V. F. Yesavage, *J. Chem. Eng. Data* **33**:138 (1988).
11. W. J. Lanum and J. C. Morris, *J. Chem. Eng. Data* **14**:93 (1969).
12. D. J. G. Irwin, R. Johnson, and R. Palepu, *Thermochim. Acta* **82**:277 (1984).
13. Y. Oshmyansky, H. J. M. Hanley, J. F. Ely, and A. J. Kidnay, *Int. J. Thermophys.* **7**:599 (1986).
14. M. Delepine, *Compt. Rend.* **126**:964 and 1033 (1898).
15. G. S. Parks, S. S. Todd, and W. A. Moore, *J. Am. Chem. Soc.* **58**:58 (1936).
16. D. A. Flanigan, V. F. Yesavage, K. S. Cerise, V. G. Niesen, and A. J. Kidnay, *J. Chem. Thermodynam.* **20**:109 (1988).
17. S. L. Randzio, D. J. Eatough, E. A. Lewis, and L. D. Hansen, *J. Chem. Thermodynam.* **20**:937 (1988).
18. S. L. Randzio, *Pure Appl. Chem.* **63**:1409 (1991).
19. D. R. Lide (ed.), *Handbook of Chemistry and Physics*, 72nd ed. (CRC Press, Boca Raton, FL, 1991), p. 3-441.
20. S. L. Randzio, J.-P. E. Grolier, and J. R. Quint, *Fluid Phase Equil.* (in press).